Spectroscopic fingerprints of carbon nitride functional groups locked-up in hydrogen bonding interactions

Valeria Lanzilotto,[1] Jose Luis Silva,[1] Teng Zhang,[1] Cesare Grazioli,[2] Matuš Stredansky,[3,4] Konstantin Simonov,[1] Erika Giangrisostomi,[5] Ruslan Ovsyannikov,[5] Monica de Simone,[4] Marcello Coreno,[2] Carlos Moyses Araujo,[1] Barbara Brena[1] and Carla Puglia[1]

[1] Department of Physics and Astronomy, Uppsala University, P.O. Box 516, 751 20 Uppsala, Sweden
[2] ISM-CNR, Istituto di Struttura della Materia - LD2 Unit, Basovizza AREA Science Park, I-34149 Trieste, Italy
[3]Department of Physics, University of Trieste, via A. Valerio 2, Trieste, Italy
[4]CNR - IOM Laboratorio Nazionale TASC, Basovizza SS-14, km 163.5, 34012 Trieste, Italy
[5] Institute for Methods and Instrumentation for Synchrotron Radiation Research, Helmholtz-Zentrum Berlin GmbH, Albert-Einstein-Straße 15, 12489 Berlin, Germany

Abstract

In this work we have investigated the effect of intermolecular H-bonding interactions on the local electronic state of functionalities (amino and priydine-like N) usually found in *graphitic* carbon nitride materials (g-C_3N_4). For doing this, we have performed a combined X-ray photoemission (XPS) and absorption (NEXAFS) spectroscopy characterization of the melamine molecule (one of the g-C_3N_4 building blocks) both in the gas phase (non-interacting system) and in the solid state (H-bonded system). As supported by theoretical simulations of XPS and NEXAFS spectra, we have found that H-bonds mainly affects the N 1s level of the amino group, leaving almost untouched that one of the N inside the aromatic ring. This is responsible for a reduction of the intrinsic chemical shift existing between the two XPS N 1s levels. The lowering of the amino N ionization energy, also influences the energy position of the corresponding resonances of the N K-edge NEXAFS spectrum; i.e. the N 1s (NH2) --> LUMO shifts to lower photon energies. Solid state absorption spectra also show the quenching of resonances related to in-plane anti-bonding orbitals entirely localized on the amino functionalities. In their place we found a new kind of resonance which can be associated with a new anti-bonding orbital now extended over multiple amino groups belonging to adjacent molecules.

Introduction

During the last few years, polymeric materials, known as *graphitic* carbon nitrides (g-C_3N_4), have been attracting enormous interest thanks to their ability to (photo)-catalyze a huge variety of chemical processes [1]. Among these, the most attractive is the solar-driven water splitting reaction for hydrogen and oxygen evolution [2]. Although, in this field, inorganic semiconductors are still holding the stage, polymeric or "soft" photo-catalysts [3] would be preferred as they combine advantages typical of solid heterogeneous photo-catalysts, such as the recyclability and the high physicochemical stability, together with the tunability of the optoelectronic properties and nature of the active sites characteristic of organic homogeneous photo-catalysts. Moreover they can be easily synthesized from inexpensive and earth-abundant precursors.
g-C_3N_4 are usually modeled as binary CN sheets based on *s*-triazine or *s*-heptazine units connected through tertiary amino-groups N-$(C)_3$ (see Fig. 1a, b). Equivalently, triamino-*s*-triazine (melamine) and triamino-*s*-heptazine (melem) can be also considered as the corresponding building blocks. Actually, g-C_3N_4 materials, as those prepared by pyrolysis of CNH precursors (cyanamide, dicyanamide, melamine, urea, thiourea), consist of amorphous powders always containing a variable amount of hydrogen (1-2 % wt) [4], [5]. The hydrogen content can indicate the presence of peripheral primary amino groups (-NH_2) and bridging -NH- amines. Indeed, g-C_3N_4 powders are most likely to be composed of *s*-heptazine/*s*-triazine based polymers with different degrees of condensation and cross-linking. However, to date, there is no way of knowing the exact composition of these materials as their amorphous nature and lack of solubility prevent the use of classical characterization techniques. In particular synthesis conditions, *Lotsch et al.* were able to isolate some side g-C_3N_4 crystalline phases and determine the corresponding structures [5], [6]. In one case, it was observed a linear polymer (melon) in which s-heptazine units are connect via -NH- bridges and preserve one primary amino group per unit (-NH_2). The chains are arranged in a zigzag-type fashion which allows medium-strong hydrogen bonding interactions (-NH••N=C) that stabilize the formation of a close-packed 2D

array (Fig. 1c). In another case, it was observed a continuous 2D heptazine network exclusively based on covalent -NH- bridges (polyheptazine imide or PHI). In this structure, the resulting large triangular void can host a single melamine molecule which is tightly anchored to the surrounding heterocycles via multiple hydrogen bonds (Fig. 1d). Despite its ill-defined nature, amorphous g-C_3N_4 powders provide higher photo-catalytic activity as compared to crystalline phases [7], [8]. Indeed, as in most heterogonous catalysts, enhancement of photo-catalytic activity is often associated with the availability of more/better exposed active sites, such as surface terminations and defects [1]. By contrast, in crystalline phases of melon or PHI, possible active sites (primary or secondary amines and pyridine-like N) are locked up in intermolecular H-bonds preventing water molecules to H-bind the N-functionalities. According to few theoretical studies based on ideal binary CN sheets [9], [10] or the s-heptazine unit [11], the interaction at the basis of the water-splitting mechanism would be the H-bond formation between the hydrogen atoms of the water molecule and the lone pair of the aromatic N. In a recent study, *Lotsch et al.* [7] have shown that also primary and secondary amines can have a role as possible active sites, as low-mass weight heptazine oligomers have been found to have up to three times the activity of ill-defined g-C_3N_4 materials. In the oligomers case, indeed, the amino groups are not only more prevalent but also better exposed as confirmed by the stacking disorder and conformational flexibility of these less condensed materials.

Despite the implications that H-bonds can have on the photo-activity of carbon nitride materials, to date, no detailed spectroscopic information are available about the hydrogen mediated interaction between the amino functional groups and the nitrogen atoms inside pyridine-like rings [12]–[15]. By contrast, H-bonded structures formed by melamine and/or melem on different kinds of surfaces have been the subject of extensive scanning tunneling microscopy and theoretical investigation [16]–[22]. Both molecules can be sublimated in ultra-high vacuum condition allowing the building up of highly pure and defect-free epitaxial films. At the monolayer regime, surfaces like Au(111) or Ag(111) afford flat adsorption and formation of peculiar honeycomb structures where amino and pyridine-like functionalities are involved in intermolecular H-bonds which are very similar to those existing in the crystalline structures of melon and PHI. Moreover, contrary to polymeric materials, these small molecules can be also studied in gas phase, which is fundamental to get access to the properties of the "non-interacting" functional groups.

To deeply understand how intra-molecular H-bonding interactions impact on the local electronic state of carbon nitride functionalities, we have exploited the high processability of the melamine molecule to perform a combined gas-phase and solid state characterization by means of core level spectroscopies, specifically X-ray photoemission spectroscopy (XPS) and near edge absorption X-ray fine structure spectroscopy (NEXAFS). Although hydrogen bonds do not determine a change in the formal oxidation state, they can largely affect the core level binding energies of the involved heteroatoms. For instance, the head-to-tail H-bonded structure observed in thin film of pyridincarboxylic acids (-C=N••HOOC) is responsible for a chemical shift of the N 1s level of about 1.7 eV relative to the non-interacting system[23]. Being an initial state effect, the change in the N 1s level binding energy also affect the energy position of the corresponding N K-edge NEXAFS resonances. The high sensitivity of XPS/NEXAFS also provides enough contrast for disentangling H-bonding effects when the shared proton is linking functional groups having the same heteroatom; i.e. clusters of carboxylic acids (C=O••HOOC)[24] or thick films of croconic acid (C=O•••HO-C)[25], [26].

In the melamine case, we have found that H-bonding interaction mainly affects the N 1s level of the amino nitrogen, which determines a reduction of the XPS chemical shift existing between the two non-equivalent N atoms. On the other hand, the electronic state of the N accepting the proton (:N=C) remains almost unperturbed, as confirmed by theoretical simulations of the N 1s binding energies obtained for both the monomer and the H-bonded system. The core level shift experienced by the amino N 1s level, also affects the N K-edge NEXAFS spectrum, moving the N1s --> LUMO transition to lower photon energy. Theoretical simulations also show that intermolecular H-bonds determine the quenching of resonances associated with transitions from the amino N 1s level to in-plane orbitals (mainly localized on the -NH_2 group) and the occurrence of a less intense resonance related to a new kind of orbital which extend from the amino N to the amino groups in the neighboring molecules.

These results show that, among the two type of N, H-bonding interactions strongly modify the local electronic state of the amino group, therefore suggesting that this functional group has to have a role in the water splitting reaction. It is reasonable to expect the also in the presence of water, the O lone pair would act as the lone pair of the triazine N. The NHH••OH••N interaction could, than, facilitates the transfer of the proton to the triazine N. Such a model could, at the same time, supports both the theoretical descriptions of the water-splitting mechanism based on the H-bond between the water and the :N-C [9]–[11], and the

experimental findings of *Lotsch et al.*[7] where the availability of primary/secondary amino groups seems to be fundamental for enhancing the photo-activity of g-C_3N_4 materials.

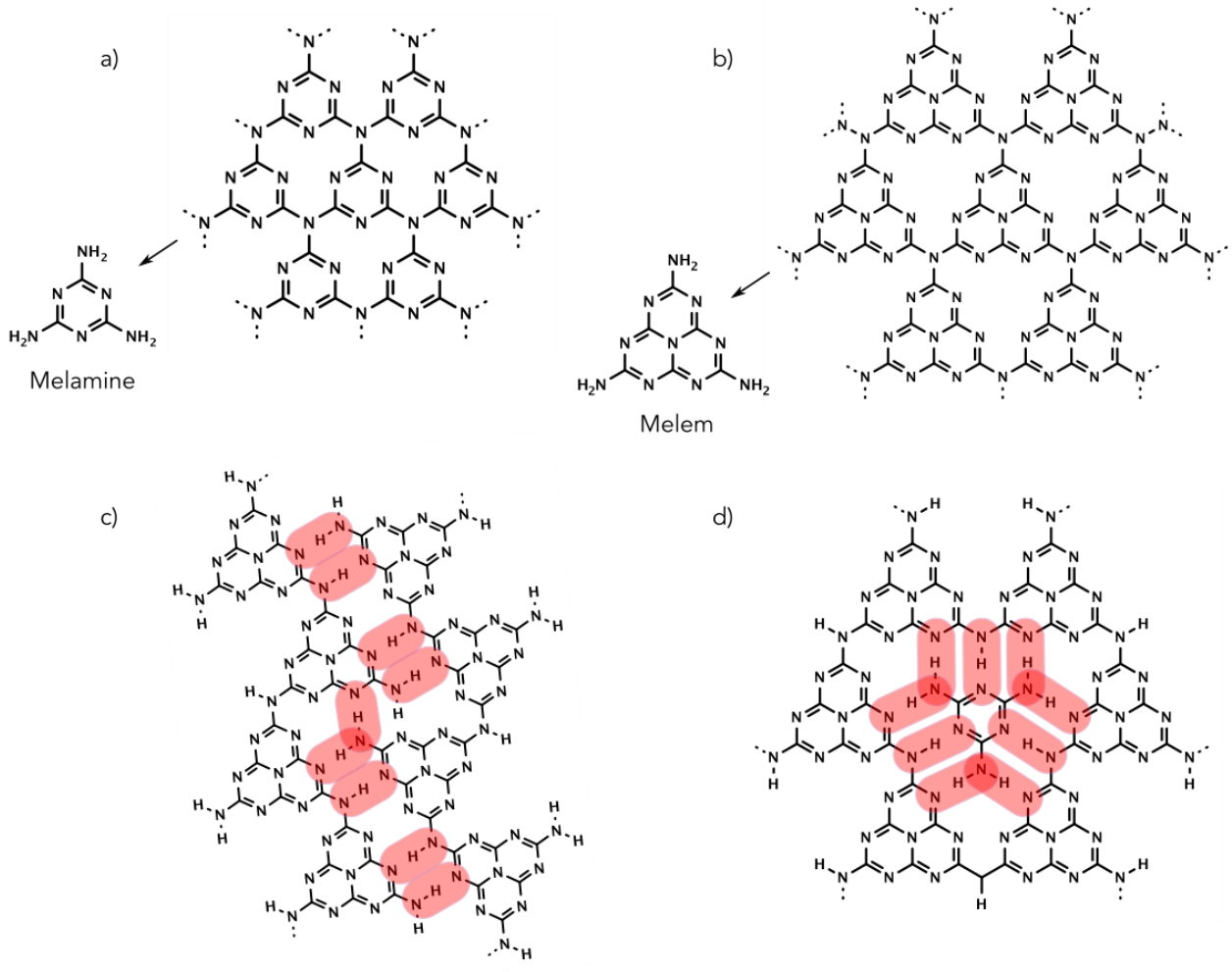

Figure 1 a, b) Postulated binary CN materials based on the building blocks melamine and melem; c) Hydrogen-bonded 2D assembly of melon chains; d) 2D continuos network of polyheptazine imide with H-bound melamine molecules.

Methods

Experimental

Gas phase measurements were performed at the non-permanent ULLA end-station installed at the GasPhase beamline of the Elettra Synchrotron (Trieste, Italy). Melamine was purchased from Sigma Aldrich (purity 99%) and sublimated from a stainless steel crucible kept at a temperature of ~ 403 K. The sublimation temperature was determined by subsequent measurements of the valence band spectrum while slowly increasing the crucible temperature. The procedure allowed a fine control of the degassing process, which was completed with the fully disappearance of the typical contamination peaks, i.e. mostly water. The XPS spectra were acquired with the Scienta SES-200 hemispherical analyzer. The C 1*s* and N 1*s* spectra were measured respectively with photon energies of 382 eV and 495 eV and an overall energy resolution of 140 and 220 meV, respectively. The calibration of the core level ionization energy scale was made thanks to the simultaneous acquisition of the C 1*s* and N 1*s* of gaseous CO_2 and N_2 and aligning them to 297.7 eV[27] and 409.9 eV[28], respectively.

The N K-edge NEXAFS spectrum was measured in total ion yield mode with a photon energy resolution set to 200 meV. The photon energy scale calibration was provided by simultaneous acquisition of the N K-edge NEXAFS spectrum of gaseous N_2 and locating the $\pi*$ ($v' = 1$) resonance at 401.10 eV[29]. The absorption intensity was normalized with the transmitted photon flux measured by a calibrated Si photodiode.

Solid state measurements were performed at the LowDose PES end-station installed at the PM4 beamline of the BESSYII Synchrotron (Berlin, Germany)[30]. Au(111) single crystal was cleaned by sputtering and annealing cycles. Melamine molecules were sublimated from a quartz crucible resistively heated by a tantalum wire. Before deposition, powders were degassed for several hours at the sublimation temperature of ~ 390 K. All samples/films shown in the paper were prepared by keeping the substrate at room temperature. A 1 ML sample (not shown) was prepared by desorbing a thick film deposited at LN_2 temperature. The corresponding N 1*s* / Au 3*d* intensity ratio was used to roughly calibrate the coverage of 1.2 ML sample, finely determined by the fitting procedure. All XPS spectra were fitted by using Voigts components. In the case of gas phase spectra, the fitting of the N 1s line was performed without any constrain leading to an NH_2/N=C intensity ratio of about 1.2 (the same value or slightly smaller (*ca.* 1.1) was found by using respectively simple Gaussians or Gaussians with a slope on the higher BE side). The NH_2 peak was found intrinsically broader than the triazine one, showing a significant Lorentzian broadening. On the other hand, the triazine component seems to be better described by a Gaussian peak. We want to remind that we do not pretend to associate the Lorentzian broadening to the core-hole lifetime, but as a mere description of the peaks. For the multilayer, the NH_2/N=C intensity ratio was initially imposed 1:1 and then left as free parameter, which again ended up to 1.2. Finally, for the 1.2 ML sample, we imposed such a ratio equal to 1.2 for both 2nd and 1st layer components. FWHMs for each type of N component are linked between second and first layer. The XPS and NEXAFS measurements were performed with a Scienta SES-100 hemispherical analyzer. The N 1*s* and C 1*s* spectra were measured at normal emission with photon energy of 500 eV and an overall energy resolution of 230 meV. The energy scale was calibrated by aligning the Au 4$f_{7/2}$ peak to the binding energy of 84.0 eV.
The N K-edge spectra have been acquired in Auger yield mode using a fixed energy window of about 20 eV centered at the kinetic energy of 372 eV. The spectra were collected with electric field polarization parallel (NI) and almost perpendicular (GI) to the surface plane (see inset of Fig. 4). The spectra were calibrated by using the Au 4*f* line measured with both 1st and 2nd order of the last photon energy of the NEXAFS spectrum.

DFT calculations

We have performed *Ab initio* calculations based on the plane wave[31] Density Functional Theory (DFT)[32], [33]. The static ions and valence electrons were handled thought the projected augmented wave method (PAW)[34] with pseudo-potentials as implemented in VASP (Vienna Ab-initio Simulation Package) code[35]–[37]. We represented the exchange and correlation interactions through the generalized gradient approximation (GGA) with Perdew-Burke-Ernzerhof (PBE) functional[38] and hybrid density functional Heyd-Scuseria-Ernzerhof (HSE06) [A. V. Krukau *et al.* J. Chem. Phys. 125 224106 (2006)]. The relaxations converged for an energy threshold of 10^{-5}eV and forces in the range of 10^{-2}eV/Å for the gas phase melamine (monomer, dimer, trimer and hexagonal packed structure) and an hexagonal packed layer of melamine adsorbed on a slab of Au(111), as shown in the Supporting Information file (Figure_SI 5). The plane wave basis cut-off energy was set to 700 eV and a large enough vacuum region of approximately 10 Å in any direction was considered for the molecules in the gas phase to isolate the species. The surface was described by three layers of Au(111) of 10x10 Au atoms each. The supercell included 14 Å of vacuum in the perpendicular direction to the surface in order to avoid residual interactions between periodic images. The surface calculations were carried with Dumped Van der Waals dispersive corrections for the charge fluctuations included through the use of DFT-D3 scheme as implemented by Grimme[39]. The Brillouin zone was sampled with Monkhorst-Pack[40] mesh K-point of 1x1x1 grid for the Gas phase and 2x2x1 for the melamine/Au(111). We have employed the Janak-Slater (JS)[41] transition state approximation to generate a half-core occupation in order to calculate the Core level (CL) Binding Energy (BE) shifts, which have been shown to provide more accurate [T12] XPS surface signatures with respect to previous reported experiments[42], [43]. We have calculated the XPS curves using Gaussian FWHMs of 0.6 eV for the core eigenvalues. The Janak-Slater (JS) approach is described by an excited half-core electron that is removed from the system, which could be interpreted as an extraction of the (half) electron to the vacuum region. We

have calculated the BEs using the final state approximation for different occupancies concerning the neutral and charged gas phase melamine, as shown in the Supporting Information file (Figure_SI 1).
The calculations of the NEXAFS spectra were performed using the DFT code StoBe \cite{StoBe} in the transition potential approach[44]. We have used the generalized gradient corrected exchange functional by Becke[45] and the correlation functional by Perdew[46]. To describe the core excited N atoms the igloo-iii triple ζ basis of Kutzelnigg, Fleischer and Schindler[47] was used. The remaining N atoms were represented by 5 electrons effective core potentials, and the C atoms by 4 electrons effective core potentials, all provided by the StoBe package. The NEXAFS spectra were calculated for the gas phase molecule and for a quadrimer of four molecules, extracted from the hexagonal structure adsorbed on the Au(111) surface, where the H bonds between adjacent molecules could be taken care of. These structures had been previously geometrically optimized by the VASP code. The total NEXAFS N K edge spectrum in the gas phase was obtained as the average of the spectra calculated for the two types of N atoms in the gas phase molecule. In the same way, the angle resolved N K-edge spectra of the molecule with the H-bonds were obtained as the average of the spectra of each. The simulated spectra were convoluted with Gaussian curves of full width at half maximum (FWHM) of 0.5 eV up to the IP, and linearly increasing to 8.0 eV for an interval of 20 eV, and constant above. The spectra were moreover shifted by 0.39 eV (the gas phase), and 0.55 eV (the quadrimer) which includes the relativistic corrections for the N atoms[48].

Results and discussion

1. N 1s XPS

Figure 2 shows the N 1*s* XPS spectra of the melamine molecule in gas phase and adsorbed on Au(111) at two different coverage, ~ 1.2 monolayer (ML) and ~ 6 ML. The top and bottom axes correspond to the gas phase and solid state energy scale, respectively. In the former case the scale is referred to the vacuum level (Ionization Energy, IE), while in the second case to the E_F of the gold substrate (Binding Energy, BE). The most striking difference between gas phase and solid state spectra is the reduced chemical shift existing between the N 1*s* levels of the two non-equivalent nitrogen atoms (the nitrogen of the amino group (-NH_2) and the nitrogen inside the triazine ring (C=N)), that goes from about 1.5 to less than 1.0 eV. When passing from the gas phase to the multilayer the N 1*s* and C 1*s* levels associated with the triazine ring shift of about 5.4 eV, which roughly correspond to the Au(111) work function[49]. On the other hand, the shift of the amino N 1*s* level is larger and amounts to about 6.1 eV. This indicates that the reduction of the chemical shift between -NH_2 and N=C is mainly due to a change in the chemical environment of the amino nitrogen (to highlight this result, the spectra are shown by aligning the triazine N component of the gas phase spectrum with that of the multilayer).
With respect to the multilayer, both N 1*s* and C 1*s* peaks of the 1.2 ML sample shift to lower binding energy because of the more efficient core-hole screening caused by the surface vicinity. Interestingly, for this sample the N 1s line is more resolved, clearly showing two components. By disentangling the contribution due to the residual 2nd layer (filled curves), we can observe that the 1st layer components almost retain the same chemical shift found in the multilayer, while their widths are considerably reduced (see Gaussian FWHMs in Table 2).

	Exp.			*Th.*
N 1*s*	-NH_2 (eV)	C=N (eV)	chem. shift ΔE (eV)	chem. shift ΔE (eV)
gas phase	405.50	403.99	1. 51	1.67
6 ML	399.38	398.53	0.85	1.16
*1.0 ML**	398.75	397.81	0.95	1.06
C 1s		C=N		
gas phase		293.39		
6ML		287.94		
*1.0 ML**		287.10		

Table 1 Ionization and binding energies of N 1*s* and C 1*s* components obtained by curve fitting. For N 1s, the chemical shift between the N=C and NH2 components is also reported, both experimental and theoretical values. (*) For 1.2 ML only BEs of the first layer components are reported.

N 1s	-NH_2	C=N
gas phase	L 0.46 G 0.46	L 0.03 G 0.62
6 ML	L 0.51 G 0.95	L 0.11 G 1.02
*1.2 ML**	L 0.58 G 0.60	L 0.13 G 0.68

Table 2 Lorentzian (L) and Gaussian (G) FWHMs (in eV) of amino and triazine N 1*s* components obtained by curve fitting.

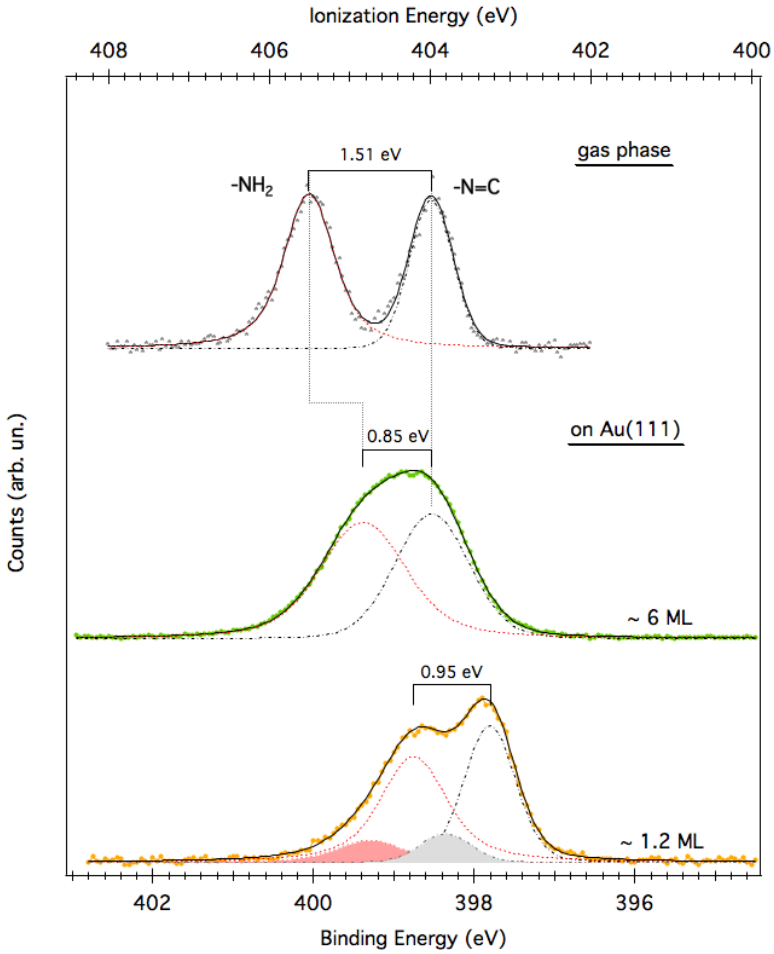

Figure 2 N 1*s* XPS region for melamine molecule in the gas phase and adsorbed on Au(111) at two different coverage, 6 ML and 1.2 ML.

Previous STM studies [16], [21] have shown that melamine adsorbs flat on Au(111) and self-assemble in honeycomb domains where amino and triazine functionalities are involved in reciprocal H-bonding interactions, i.e. NHH••N=C. Such intermolecular H-bonds, which are absent in the gas phase, are likely to be responsible for the lowering of the ionization energy of the amino N 1s level, observed both in the multilayer and monolayer samples.

To deeper investigate the hydrogen-bonding effect on the local electronic state of both functional groups, we have performed N 1*s* core level binding energy simulations for gas phase melamine and for H-bonded structures having an increasing number of melamine units. We have considered a dimer, a trimer and a *periodic* hexagonal arrangement, the latter resembling the honeycomb domains observed by STM[16][21]. The results are shown in Figure 3 along with the models of the molecular structures. As we are mainly interested in relative chemical shifts, we have arbitrarily chosen as our reference the energy scale of the monomer and shifted the other spectra in order to match the peak located at lower BE. The same peak has

been used for intensity normalization. Starting with the N 1*s* level of the monomer, we can recognize a clear similarity with the experimental XPS N 1*s* spectrum acquired for gaseous melamine. The two spectra slightly differ for the magnitude of the chemical shift, 1.67 eV (theory) *vs.* 1.51 eV (experiment). The comparison also highlights some other experimental features that are not taken into account by the calculation. For instance, the NH_2 peak is intrinsically broader than the N=C component, probably as a consequence of a more extended vibrational structure[50]. Moreover, according to our fitting procedure (i.e. Voigt components without any constrains), the intensity ratio is slightly in favor of the NH_2 component (~ 1.2). The same value is also obtained by using simple Gaussians, and slightly lower (~ 1.1) by using Gaussians with a slope for the higher BE side. These results confirm that part of the intensity associated with the aromatic nitrogen is lost and possibly spread among the weak shake-up features observed on the higher BE side (see Figure_SI 3).
When considering the dimer, we notice that the double H-bonded structure mainly breaks the equivalence of the amino N atoms, leaving almost unperturbed the N atoms inside the ring. The amino N directly involved in the H-bonds (highlighted in red) significantly shifts to lower binding energy of 0.7 eV (*avg.*), relative to the peripheral amino groups. On the other hand, the N=C counterpart (highlighted in green) shifts to higher binding energy of only 0.1 eV in average, compared to the non-interacting N=C. Such findings fully corroborate our previous conclusions simply derived by observing the energy difference between the experimental IE and BE, Δ(IE-BE), of the two N 1s levels. Similar results were also observed in the theoretical study of *Garcia-Gil et al*.[51], where, through the screening of several H-bonded molecular structures, they found the BE of the H-donor to be much more affected compared to that of the H-acceptor.
By increasing the number of melamine units, i.e. in the trimer, the weight of the NHH component increases, becoming almost comparable with that one of the free amino groups (4 : 5). Small variations of the H-bond distance, and in particular, of the N-H••N angle are responsible for the large spread in the BE values observed for NHH component (see Figure_SI 4). When considering the periodic hexagonal structure of Figure 3d, where all functional groups are locked-up in the H-bonds, the corresponding N 1s spectrum only features two components like in the monomer case but with a smaller chemical shift of 1.16 eV, which means a lowering of 0.51 eV (see Table 1). These values are not too far from those observed experimentally when passing from gaseous melamine (1.51 eV) to the thick film (0.85 eV), with a reduction of 0.66 eV (see Table 1). In the experimental spectrum, the impossibility to resolve the two components is due not only to a smaller chemical shift but mainly to the significant Gaussian broadening of the two components that can be associated with a plethora of slightly non-equivalent N atoms. Although a floating single layer with hexagonal structure successfully works as a model for the multilayer, the latter, probably, would be better described by a model comprising more than one layer (or even the crystallographic structure) where more than one type **NHH**••N=C or NHH••**N=C** are likely to be present. The case of the trimer can give an indication of the spreading of the BEs values caused by small differences in the H-bond distances and angles.

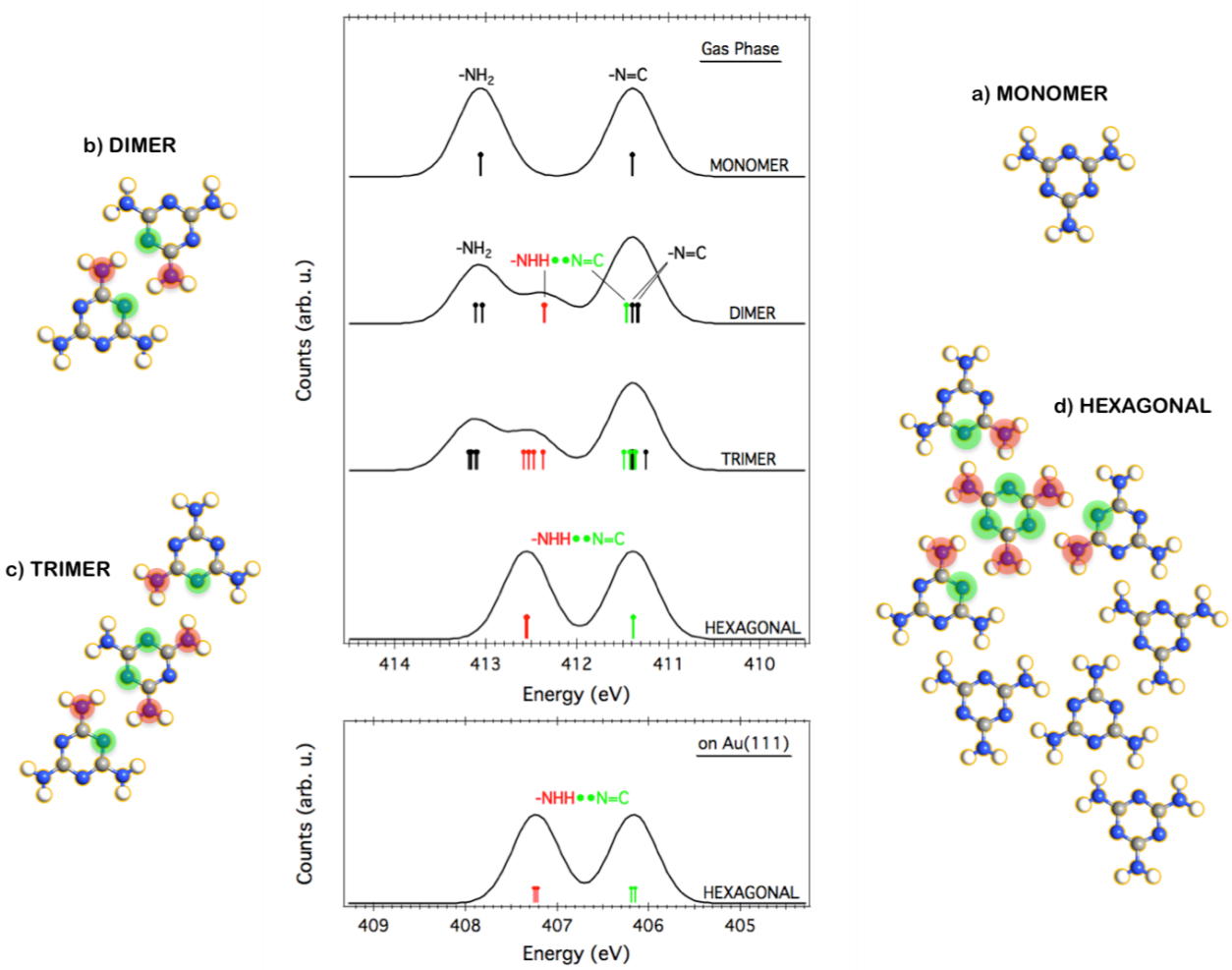

Figure 3 (Top graph) Simulated N 1*s* core level spectra for a) melamine monomer, b) dimer, c) trimer and d) a periodic hexagonal structure. (Bottom graph) Simulated N 1*s* core level spectrum for the hexagonal structure on top the Au(111) surface.

As a final step, we have also calculated the N 1s spectrum for the hexagonal layer on top the Au(111) surface that, in this case, is very close to the experimental arrangement found for the monolayer phase. Interestingly, the hexagonal structure in contact with the gold surface remains almost unperturbed compared to the "floating" layer. The only change is a slight breaking of the equivalence among both kinds of N atoms that determines a further decrease (0.1 eV) of the average chemical shift (see Table 1 and Supporting Information file for further details). At variance with the multilayer, the homogeneity of the monolayer leads to a better agreement between the theoretical and experimental chemical shift: 1.06 eV vs 0.95 eV for the monolayer and 1.16 eV vs 0.85 eV for the multilayer. Further evidence of a gained homogeneity for the monolayer, is the reduced broadening of both Gaussian components that allows to resolve the two peaks (Fig. 2).

2. N K-edge NEXAFS

Figure 4 shows the N K-edge NEXAFS spectra corresponding to the three samples already introduced in the XPS section: gas phase (gray trace), multilayer (light and dark green traces) and 1.2 ML (light and dark yellow traces). Solid state measurements have been performed at two different scattering geometries (see inset), at normal incidence (NI, electric field vector $\vec{E}$ parallel to the surface plane) and grazing incidence (GI, electric field vector $\vec{E}$ almost perpendicular to the surface plane). As melamine adsorbs flat in both films (a bit less in the multilayer), enhancement of π^* and σ^* resonances occurs at GI and NI, respectively. For a better comparison, the spectra have been aligned relative to the first resonance by shifting the gas phase spectrum of + 0.20 eV.

The π^* energy region of gaseous melamine shows three main resonances peak **a**, **b**, **c** together with a small contribution deriving from the N K-edge spectrum of residual gaseous N_2.

When considering the molecular films, both peak **a** and peak **c** can be easily recognized in the spectra taken at grazing incidence (GI). On the other hand, peak **b** seems to be vanished with the concurrent appearance of two new resonances aside peak **a** and peak **c**, marked with arrows in the spectrum acquired for the 6 ML sample. For 1.2 ML sample, the shoulder aside peak **a** is clearly visible while the one close to peak **c** seems to be hidden in the decreasing background, usually recorded at this scattering geometry and particularly enhanced because of the low coverage. The latter is also responsible for the worst S/N ratio of the NI spectrum, although it was acquired 3 times more compared to the thick film.

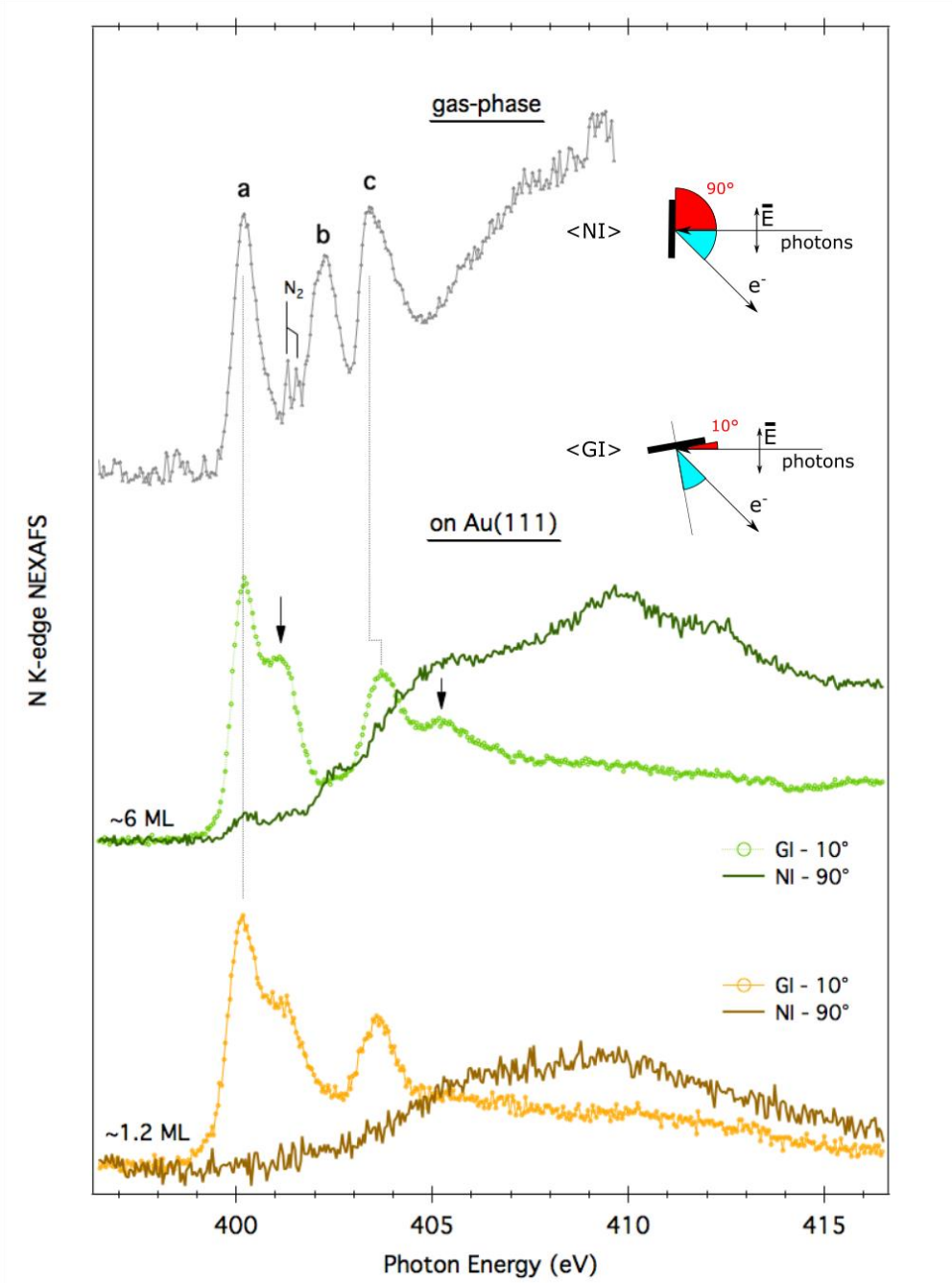

Figure 4 N K-edge NEXAFS spectra of melamine in the gas phase (gray trace) and adsorbed on Au(111) with coverage of ~ 6 ML (greenish traces) and ~ 1.2 ML (yellowish traces). The solid state measurements have been performed in two different scattering geometries: at normal incidence (NI, electric filed vector $\bar{E}$ parallel to the surface plane) and at grazing incidence (GI, electric filed vector $\bar{E}$ almost perpendicular to the surface plane). A schematic of the scattering geometry is shown in the inset.

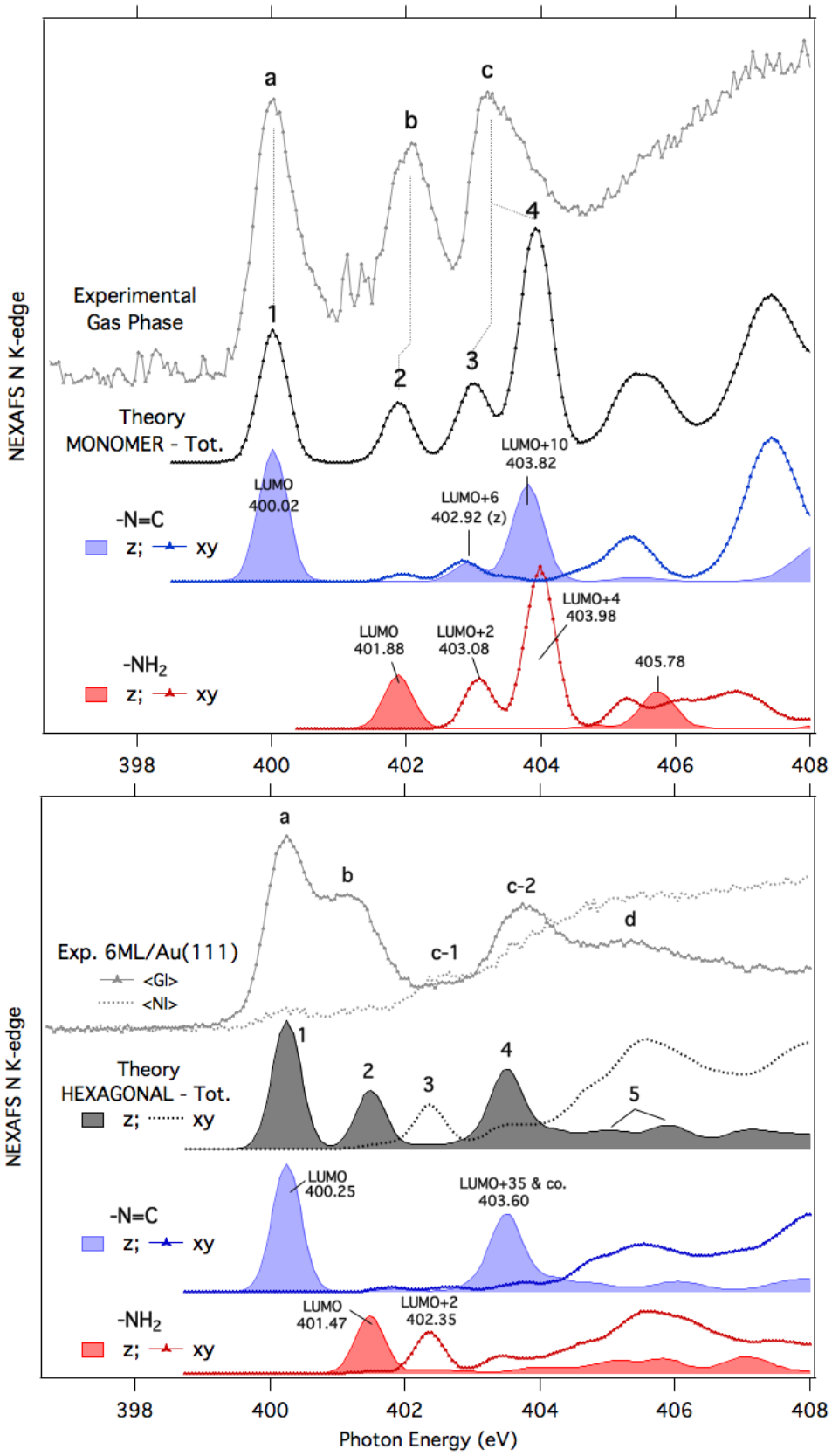

Figure 5 (Top Graph) Comparison between the experimental and theoretical NEXAFS N K-edge spectrum for isolated melamine. The theoretical spectrum has been decomposed in the contribution deriving from each N atom. Out-of-plane (z) and in-plane (xy) components are also shown. The theoretical curves have been shifted of +0.39 to align for the first resonances. (Bottom graph) Comparison between the experimental N K-edge spectra taken at GI and NI for the 6 ML sample and the out-of-plane component of the N K-edge spectrum simulated for a floating hexagonal layer. For the energy alignment of the first resonance, the theoretical spectra have been shifted of +0.55.

To better understand the relationships existing between the features of the gas phase and films spectra, we have performed theoretical modeling of the N K-edge NEXAFS for both the monomer (gas phase) and a group of four molecules extracted from the H-bonded hexagonal structure adsorbed on the Au(111) (HB model). In Figure 5 (top panel) we compare the gas phase results with the total N K-edge spectrum computed for the monomer (theoretical curve has been shifted of +0.39 eV). In the same figure we have also plotted separately the in-plane and out-of plane contribution for each type of N atom. As for the HB model, we have computed the in-plane and out-of-plane spectra and compared them, respectively, to the GI and NI spectra of the 6 ML sample (bottom panel of Figure 5; theoretical curves has been shifted of +0.55 eV). Also in this case, each spectrum has been further decomposed in the contribution deriving from triazine and amino N. For the comparison with the HB model, the thick film spectra have been preferred to those of the 1.2 ML sample since the formers clearly show all the new features deriving from the H-bonding interaction. As it can be seen the shape of the theoretical curves is in very good agreement with the corresponding experimental NEXAFS profile. By analyzing the in-plane and out-of-plane contribution of each N atom for the monomer and the HB model, we are able to clarify the overall effect of the HB network on the unoccupied electronic structure of the melamine molecule.

Starting with the analysis of the monomer, we can firstly identify the nature of the main resonances: peak **a** is entirely associated with a transition from the triazine N 1s level (N=C) to the lowest molecular orbital, LUMO (peak **1**). Equivalently, peak **b** corresponds to a transition from the amino N 1s level (-NH_2) to the LUMO (peak **2**). The energy separation between peak 1 and peak 2 is about 1.85 eV, very close to the core level shift between the two N atoms 1.67 eV (theory). The third resonance (peak **c**) corresponds to peak **3** and peak **4**, both deriving from the overlap of two different kinds of transitions. One is the excitation from the triazine N 1s level towards the LUMO+6 and LUMO+10 orbitals of π^* character (at 402.92 eV and 403.82 eV respectively), and the second one is the excitation from the amino N 1s level to anti-bonding orbitals of σ^* character localized on the amino groups, the LUMO+2 and LUMO+4 (at 403.08 eV and 403.98 eV respectively). The iso-surfaces of all aforementioned orbitals are shown in Figure 6.

Turning now to the four-molecule HB model, we can see that the three main peaks in the theoretical out-of-plane spectrum (peaks **1, 2, 4**) follow well the profile of the experimental GI spectrum. The decomposition of the spectrum in the NH_2 and N=C contributions, clearly shows that both peak **1/a** peak **2/b** have, indeed, the same origin as in the monomer case although peak **2/b** is now significantly shifted to lower photon energies. Such a shift is just a consequence of the the reduction of the amino N 1s ionization energy, as observed through the analysis of the XPS data (Fig. 3). The energy separation between peak 1 and peak 2 is now 1.22 eV, which is very close to the theoretical energy difference of 1.16 eV between the corresponding core levels. The third out-of-plane peak, peak **4/c-2**, has only contribution from the triazine N, and derives from several transitions to orbitals of π^* character which are clustered around a slightly more intense component at 403.60 eV (corresponding to the LUMO+35). This orbital has the same symmetry and shape as the LUMO+10 of the monomer that contributes to about 50% to peak 4 (see again top panel of Fig. 5). Finally, the out-of-plane component of the amino N at about 405.78 eV in the monomer simulation, is not clearly discernable in the HB model. In its place we found several smaller contributions that summed up with the triazine counterpart give rise to the peak **5/d**.

As for the NI spectrum (in-plane contributions), one small resonance is obtained in the theory at about 402.35 eV (peak **3**), probably corresponding to the experimental peak labeled as **c-1**. According to our calculations, this peak is related to a transition from the amino N 1s level to the LUMO+2, a σ^* orbital that involves the amino N and its H atoms, and extends towards the two molecules close by. Such orbital can be regarded as a modification of the LUMO+2 and LUMO+4 previously found for the monomer. Respect to the monomer, this new transition is shifted to lower photon energy (probably an effect of the reduced amino N 1s IE) and has much lower intensity. The quenching of xy-transitions involving the amino N seems to be a recurring effect in the N K-edge spectra of NH_2-containing benzene derivatives when passing from the gas phase to the solid state [52].

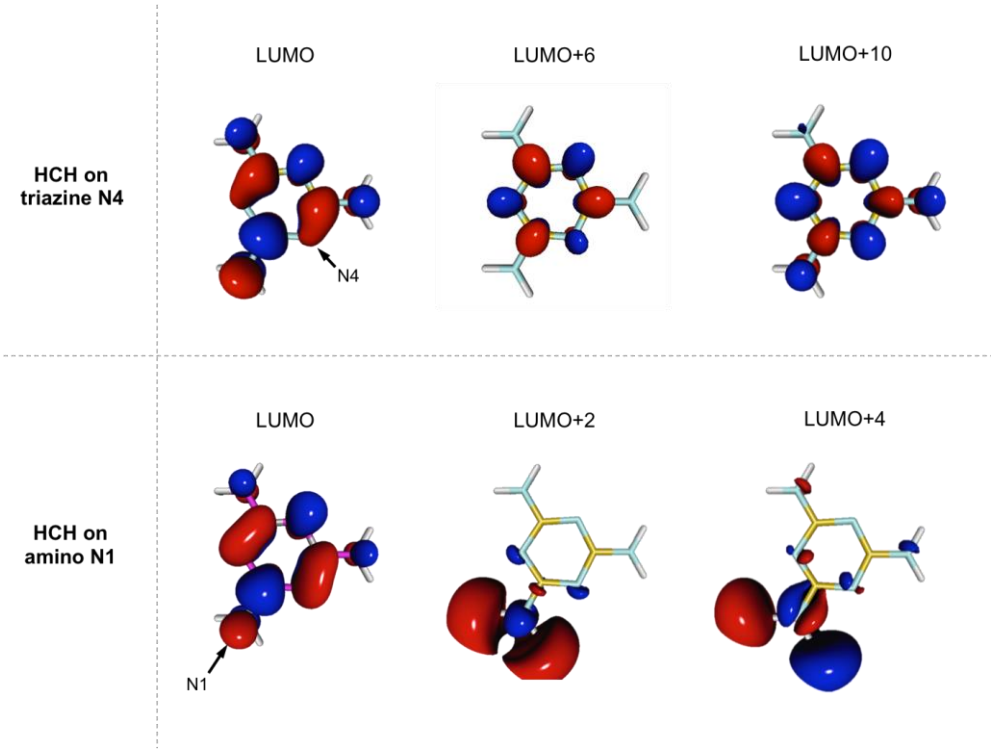

Figure 6 Representation of the main LUMOs as probed in the N K-edge spectrum of isolated melamine.

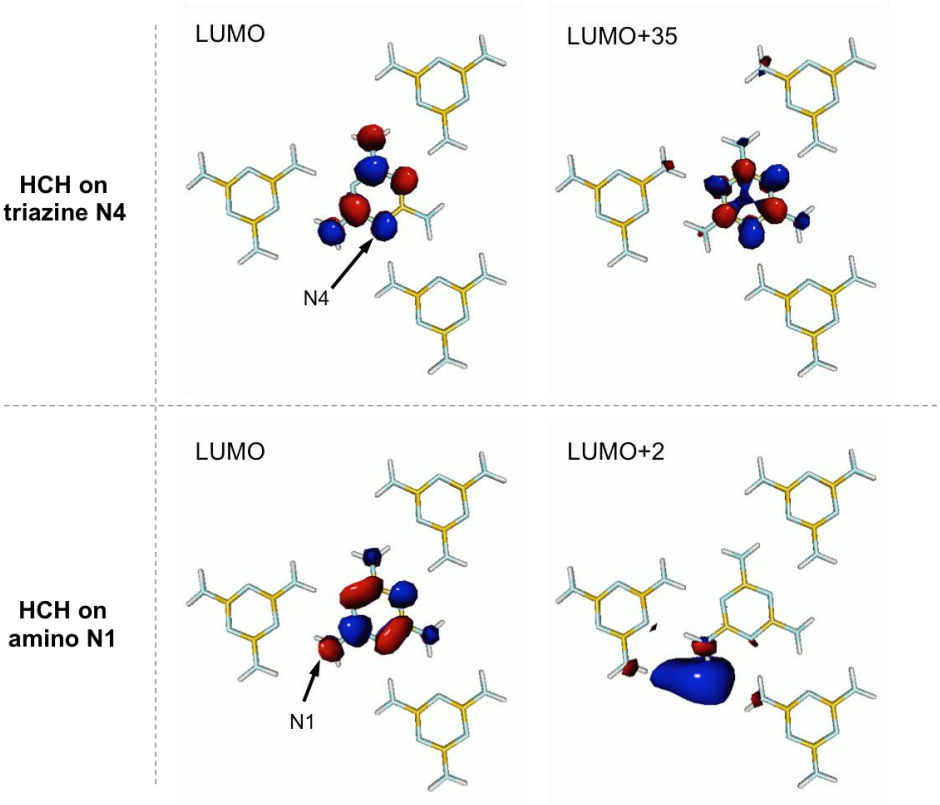

Figure 7 Representation of the main LUMOs as probed in the N K-edge spectrum of H-bonded melamine.

Conclusions

In conclusion, we have shown that intermolecular H-bonding interactions mainly affect the the N 1s level of the amino group, leaving almost unperturbed that one of the triazine N. As a consequence, the chemical shift between the two N atoms is significantly reduced respect to the non-interacting system. The reduction of the

ionization energy of the amino N 1s, also affects the energy position of the corresponding resonances in the N K-edge NEXAFS spectrum, i.e. the N 1s (NH2) --> LUMO transition shifts to lower photon energies. Solid state absorption spectra also show the quenching of transitions involving in-plane anti-bonding orbitals entirely localized on the -NH_2 terminations. In their place, we found a new kind of transition which is instead associated with a σ* orbital on the amino group and extended on those of the neighboring molecules.

Supporting Information

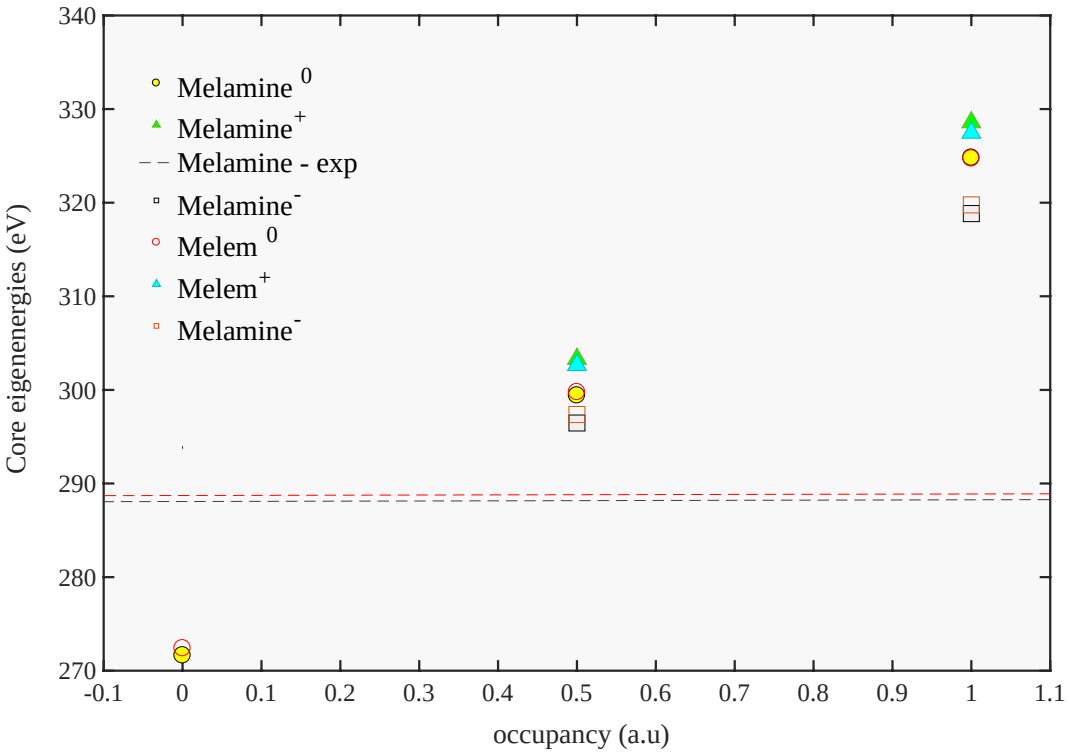

Figure_SI 1 C 1s core eigenenergies for different charged systems and occupancies which shows a linear behavior and better fitting of the half core occupation approach in comparison with the experimental result.

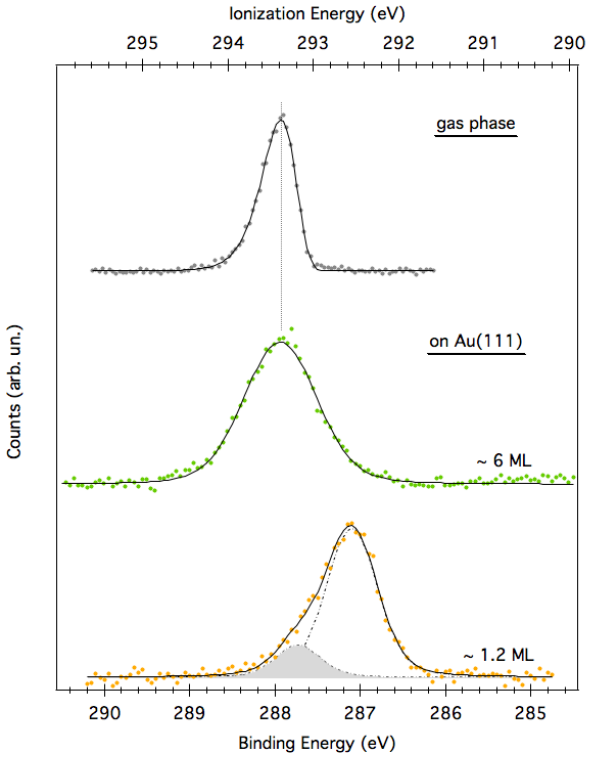

Figure_SI 2 C 1*s* XPS spectra (plus curve fitting) of gaseous melamine and melamine films adsorbed on Au(111).

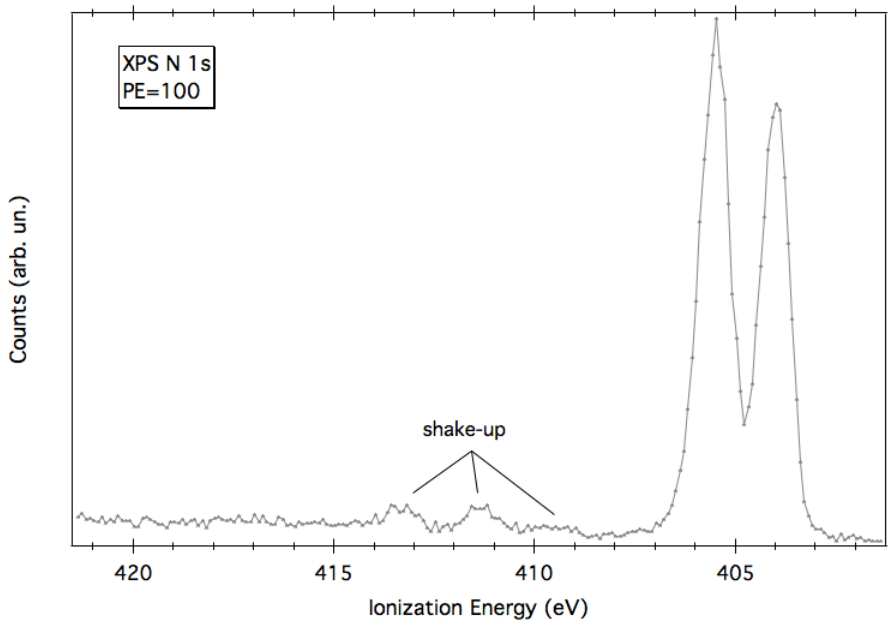

Figure_SI 3 N1s XPS spectrum of gaseous melamine including shake-up satellites.

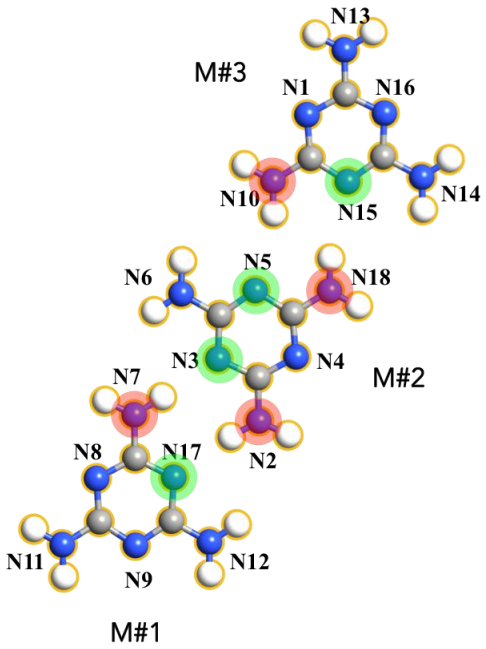

H-bond		BE (eV) -NH_2	BE (eV) -C=N	ΔE (eV)
(N10)-H••N5 Angle	2.202 Å 175.57°	412.53	411.30	1.23
(N18)-H••N15 Angle	2.195 Å 176.23°	412.47	411.36	1.11
(N7)-H••N3 Angle	2.035 Å 176.17°	412.41	411.31	1.10
(N2)-H••N17 Angle	1.964 Å 177.12°	412.32	411.42	0.9

Figure_SI 4 Trimer structure along with details about H-bond distances, angles, BEs and chemical shifts.

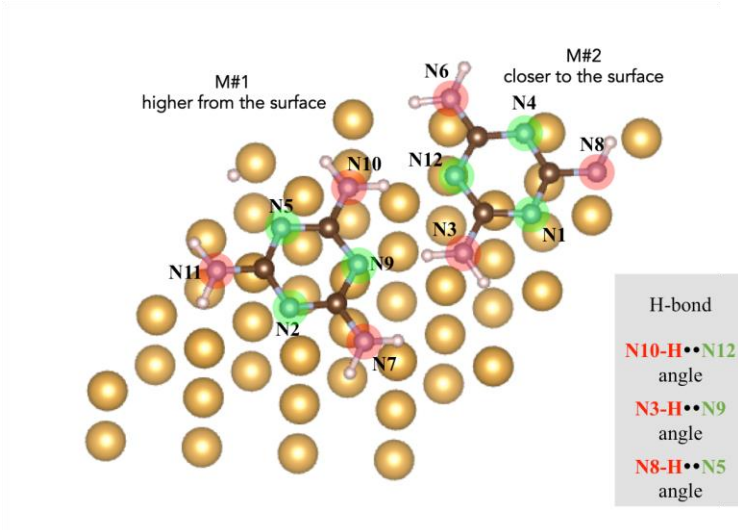

M#1	Z (Å)	M#2	Z (Å)
N9	11.31	N12	11.25
N2	11.32	N4	11.27
N5	11.31	N1	11.25
N10	11.31	N3	11.21
N7	11.32	N6	11.26
N11	11.32	N8	11.24

H-bond		BE (eV) -NH_2	BE (eV) -C=N	ΔE(eV)
N10-H••N12 angle	2.086 Å 174.56°	407.25	406.15	1.1
N3-H••N9 angle	2.045 Å 174.94°	407.21	406.18	1.03
N8-H••N5 angle	2.038 Å -	407.23	406.19	1.04

Figure_SI 5 Hexagonal layer on top the Au(111) surface. Top table lists the Z position of amino and triazine N atoms. Bottom table lists details about H-bond distances, angles, BEs and chemical shifts.

References

[1] Y. Wang, X. Wang, and M. Antonietti, "Polymeric Graphitic Carbon Nitride as a Heterogeneous Organocatalyst: From Photochemistry to Multipurpose Catalysis to Sustainable Chemistry," *Angew. Chemie Int. Ed.*, vol. 51, pp. 68–89, 2012.

[2] X. Wang, K. Maeda, A. Thomas, K. Takanabe, G. Xin, J. M. Carlsson, K. Domen, and M. Antonietti, "A metal-free polymeric photocatalyst for hydrogen production from water under visible light.," *Nat. Mater.*, vol. 8, no. 1, pp. 76–80, 2009.

[3] V. S. Vyas, V. W. Lau, and B. V Lotsch, "Soft Photocatalysis : Organic Polymers for Solar Fuel Production," *Chem. Mater.*, vol. 28, pp. 5191–5204, 2016.

[4] A. Schwarzer, T. Saplinova, and E. Kroke, "Tri-s-triazines (s-heptazines) — From a 'mystery molecule' to industrially relevant carbon nitride materials," *Coord. Chem. Rev.*, vol. 257, pp. 2032–2062, 2013.

[5] B. V Lotsch, M. Dçblinger, J. Sehnert, L. Seyfarth, J. Senker, O. Oeckler, and W. Schnick, "Unmasking Melon by a Complementary Approach Employing Electron Diffraction , Solid-State NMR Spectroscopy , and Theoretical Calculations — Structural Characterization of a Carbon Nitride Polymer," *Chem. - A Eur. J.*, vol. 13, pp. 4969–4980, 2007.
[6] B. V Lotsch, J. Wack, and W. Schnick, "Structure elucidation of polyheptazine imide by electron diffraction — a templated 2D carbon nitride network," *Chem. Commun.*, pp. 1541–1543, 2009.
[7] V. W. Lau, M. B. Mesch, V. Duppel, V. Blum, J. Senker, and B. V Lotsch, "Low-Molecular-Weight Carbon Nitrides for Solar Hydrogen Evolution," *J. Am. Chem. Soc.*, vol. 137, pp. 1064–1072, 2015.
[8] V. W. Lau, I. Moudrakovski, T. Botari, S. Weinberger, M. B. Mesch, V. Duppel, J. Senker, V. Blum, and B. V Lotsch, "Rational design of carbon nitride photocatalysts by identification of cyanamide defects as catalytically relevant sites," *Nat. Commun.*, vol. 7, p. 12165, Jul. 2016.
[9] J. Wirth, R. Neumann, M. Antonietti, and P. Saalfrank, "Adsorption and photocatalytic splitting of water on graphitic carbon nitride: a combined first principles and semiempirical study," *Phys. Chem. Chem. Phys.*, vol. 16, no. 30, pp. 15917–15926, 2014.
[10] H.-Z. Wu, L.-M. Liu, and S.-J. Zhao, "The effect of water on the structural, electronic and photocatalytic properties of graphitic carbon nitride," *Phys. Chem. Chem. Phys.*, vol. 16, no. 7, p. 3299, 2014.
[11] J. Ehrmaier, T. N. V. Karsili, A. L. Sobolewski, and W. Domcke, "Mechanism of Photocatalytic Water Splitting with Graphitic Carbon Nitride: Photochemistry of the Heptazine-Water Complex," *J. Phys. Chem. A*, vol. 121, no. 25, pp. 4754–4764, 2017.
[12] Y. P. Lin, O. Ourdjini, L. Giovanelli, S. Clair, T. Faury, Y. Ksari, J. M. Themlin, L. Porte, and M. Abel, "Self-assembled melamine monolayer on Cu(111)," *J. Phys. Chem. C*, vol. 117, no. 19, pp. 9895–9902, 2013.
[13] W. J. Doherty, S. L. Sorensen, and R. Friedlein, "Selective hydrogen bond disruption in adenine monolayer films by reaction with water," *J. Electron Spectros. Relat. Phenomena*, vol. 174, no. 1–3, pp. 107–109, 2009.
[14] A. P. Dementjev, A. De Graaf, M. C. M. Van De Sanden, and K. I. Maslakov, "X-Ray photoelectron spectroscopy reference data for identification of the C 3N4 phase in carbon-nitrogen films," *Diam. Relat. Mater.*, vol. 9, pp. 1904–1907, 2000.
[15] M. Ruiz-Osés, T. Kampen, N. González-Lakunza, I. Silanes, P. M. Schmidt-Weber, A. Gourdon, A. Arnau, K. Horn, and J. E. Ortega, "Spectroscopic fingerprints of amine and imide functional groups in self-assembled monolayers.," *Chemphyschem a Eur. J. Chem. Phys. Phys. Chem.*, vol. 8, no. 11, pp. 1722–6, Aug. 2007.
[16] F. Silly, A. Q. Shaw, M. R. Castell, G. A. D. Briggs, M. Mura, N. Martsinovich, and L. Kantorovich, "Melamine structures on the Au(111) surface," *J. Phys. Chem. C*, vol. 112, no. 30, pp. 11476–11480, 2008.
[17] M. Mura, N. Martsinovich, and L. Kantorovich, "Theoretical study of melamine superstructures and their interaction with the Au(111) surface," *Nanotechnology*, vol. 19, no. 46, p. 465704, 2008.
[18] C. H. Schmitz, J. Ikonomov, and M. Sokolowski, "Two commensurate hydrogen-bonded monolayer structures of melamine on Ag(111)," *Surf. Sci.*, vol. 605, no. 1–2, pp. 1–6, 2011.
[19] J. Eichhorn, S. Schlögl, B. V. Lotsch, W. Schnick, W. M. Heckl, and M. Lackinger, "Self-assembly of melem on Ag(111) - emergence of porous structures based on amino-heptazine hydrogen bonds," *CrystEngComm*, vol. 13, p. 5559, 2011.
[20] S. Uemura, M. Aono, T. Komatsu, and M. Kunitake, "Two-dimensional self-assembled structures of melamine and melem at the aqueous solution-Au(111) interface," *Langmuir*, vol. 27, no. 4, pp. 1336–1340, 2011.
[21] W. Li, S. H. I. He-xia, W. Wen-yuan, S. Hong, and X. Shao, "Identifying the Hydrogen

Bonding Patterns of Melamine and Melem Self-Assemblies on Au (111) Surface," *Acta Phys.-Chim. Sin.*, vol. 33, no. 2, pp. 393–398, 2017.
[22] M. Bao, X. Wei, L. Cai, Q. Sun, Z. Liu, and W. Xu, "Self-assembly of melem on Au(111) and Ag(111): the origin of two different hydrogen bonding configurations," *Phys. Chem. Chem. Phys.*, vol. 19, pp. 18704–18708, 2017.
[23] J. N. O'Shea, Y. Luo, J. Schnadt, L. Patthey, H. Hillesheimer, J. Krempasky, D. Nordlund, M. Nagasono, P. A. Brühwiler, and N. Mårtensson, "Hydrogen-Bond Induced Surface Core-Level Shift in pyridine carboxylic acids," *Surf. Sci.*, vol. 486, pp. 157–166, 2001.
[24] K. Tabayashi, O. Takahashi, H. Namatame, and M. Taniguchi, "Substituent R-effects on the core-electron excitation spectra of hydrogen-bonded carboxylic-acid (R-COOH) clusters: Comparison between acetic-acid and formic-acid clusters," *Chem. Phys. Lett.*, vol. 557, pp. 1–9, 2013.
[25] F. Bisti, A. Stroppa, S. Picozzi, and L. Ottaviano, "Fingerprints of the hydrogen bond in the photoemission spectra of croconic acid condensed phase: An x-ray photoelectron spectroscopy and ab-initio study," *J. Chem. Phys.*, vol. 134, no. 17, 2011.
[26] F. Bisti, A. Stroppa, F. Perrozzi, M. Donarelli, S. Picozzi, M. Coreno, M. De Simone, K. C. Prince, and L. Ottaviano, "The electronic structure of gas phase croconic acid compared to the condensed phase: More insight into the hydrogen bond interaction," *J. Chem. Phys.*, vol. 138, no. 1, pp. 1–5, 2013.
[27] V. Myrseth, J. D. Bozek, E. Kukk, L. J. Sathre, and T. D. Thomas, "Adiabatic and vertical carbon 1s ionization energies in representative small molecules," *J. Electron Spectros. Relat. Phenomena*, vol. 122, no. 1, pp. 57–63, 2002.
[28] A. A. Bakke, H. W. Chen, and W. L. Jolly, "A table of absolute core-electron binding-energies for gaseous atoms and molecules," *J. Electron Spectros. Relat. Phenomena*, vol. 20, no. 3, pp. 333–366, 1980.
[29] R. N. S. Sodhi and C. E. Brion, "Reference energies for inner shell electron energy-loss spectroscopy," *J. Electron Spectros. Relat. Phenomena*, vol. 34, no. 4, pp. 363–372, Jan. 1984.
[30] E. Giangrisostomi, R. Ovsyannikov, F. Sorgenfrei, T. Zhang, A. Lindblad, Y. Sassa, U. B. Cappel, T. Leitner, R. Mitzner, S. Svensson, N. Mårtensson, and A. Föhlisch, "Low Dose Photoelectron Spectroscopy at BESSY II: Electronic structure of matter in its native state," *J. Electron Spectros. Relat. Phenomena*, p. http://dx.doi.org/10.1016/J.elspec.2017.05.011, 2017.
[31] M. C. Payne, M. P. Teter, D. C. Allan, T. A. Arias, and J. D. Joannopoulos, "Iterative minimization techniques for ab initio total-energy calculations: molecular dynamics and conjugate gradients," *Rev. Mod. Phys.*, vol. 64, no. 4, pp. 1045–1097, Oct. 1992.
[32] W. Kohn and L. J. Sham, "Self-Consistent Equations Including Exchange and Correlation Effects," *Phys. Rev.*, vol. 140, no. 4A, pp. A1133–A1138, Nov. 1965.
[33] R. O. Jones and O. Gunnarsson, "The density functional formalism, its applications and prospects," *Rev. Mod. Phys.*, vol. 61, no. 3, pp. 689–746, Jul. 1989.
[34] P. E. Blöchl, "Projector augmented-wave method," *Phys. Rev. B*, vol. 50, no. 24, pp. 17953–17979, Dec. 1994.
[35] G. Kresse and J. Hafner, "Ab initio molecular dynamics for open-shell transition metals," *Phys. Rev. B*, vol. 48, no. 17, pp. 13115–13118, Nov. 1993.
[36] G. Kresse and J. Furthmüller, "Efficient iterative schemes for ab initio total-energy calculations using a plane-wave basis set," *Phys. Rev. B*, vol. 54, no. 16, pp. 11169–11186, Oct. 1996.
[37] G. Kresse and D. Joubert, "From ultrasoft pseudopotentials to the projector augmented-wave method," *Phys. Rev. B*, vol. 59, no. 3, pp. 1758–1775, Jan. 1999.
[38] J. Perdew, K. Burke, and M. Ernzerhof, "Generalized Gradient Approximation Made Simple.," *Phys. Rev. Lett.*, vol. 77, no. 18, pp. 3865–3868, Oct. 1996.

[39] S. Grimme, “Semiempirical GGA-type density functional constructed with a long-range dispersion correction,” *J. Comput. Chem.*, vol. 27, no. 15, pp. 1787–1799, Nov. 2006.
[40] J. D. Pack and H. J. Monkhorst, “Special points for Brillouin-zone integrations—a reply,” *Phys. Rev. B*, vol. 16, no. 4, pp. 1748–1749, Aug. 1977.
[41] J. F. Janak, “Proof that ∂E / ∂n_i = ε in density-functional theory,” *Phys. Rev. B*, vol. 18, no. 12, pp. 7165–7168, Dec. 1978.
[42] N. Pueyo Bellafont, F. Viñes, W. Hieringer, and F. Illas, “Predicting core level binding energies shifts: Suitability of the projector augmented wave approach as implemented in VASP,” *J. Comput. Chem.*, vol. 38, no. 8, pp. 518–522, Mar. 2017.
[43] R. C. Salvarezza and P. Carro, “Exploring the core level shift origin of sulfur and thiolates on Pd(111) surfaces,” *Phys. Chem. Chem. Phys.*, vol. 17, no. 37, pp. 24349–24355, 2015.
[44] L. Triguero, L. G. M. Pettersson, and H. Ågren, “Calculations of near-edge x-ray-absorption spectra of gas-phase and chemisorbed molecules by means of density-functional and transition-potential theory,” *Phys. Rev. B*, vol. 58, no. 12, pp. 8097–8110, Sep. 1998.
[45] A. D. Becke, “Density-functional exchange-energy approximation with correct asymptotic behavior,” *Phys. Rev. A*, vol. 38, no. 6, pp. 3098–3100, Sep. 1988.
[46] J. P. Perdew, “Density-functional approximation for the correlation energy of the inhomogeneous electron gas,” *Phys. Rev. B*, vol. 33, no. 12, pp. 8822–8824, Jun. 1986.
[47] W. Kutzelnigg, U. Fleischer, and M. Schindler, “The IGLO-Method: Ab-initio Calculation and Interpretation of NMR Chemical Shifts and Magnetic Susceptibilities,” Springer, Berlin, Heidelberg, 1990, pp. 165–262.
[48] L. Triguero, O. Plashkevych, L. G. M. Pettersson, and H. Ågren, “Separate state vs. transition state Kohn-Sham calculations of X-ray photoelectron binding energies and chemical shifts,” *J. Electron Spectros. Relat. Phenomena*, vol. 104, no. 1–3, pp. 195–207, Jul. 1999.
[49] S. Hüfner, *Photoelectron Spectroscopy, Principles and Applications*. Springer, 2003.
[50] H. Ågren, J. Müller, and J. Nordgren, “Vibrational excitations in soft x-ray emission and core ESCA spectra of NH3,” *J. Chem. Phys.*, vol. 72, no. 7, pp. 4078–4083, 1980.
[51] S. Garcia-Gil, A. Arnau, and A. Garcia-Lekue, “Exploring large O 1s and N 1s core level shifts due to intermolecular hydrogen bond formation in organic molecules,” *Surf. Sci.*, vol. 613, pp. 102–107, Jul. 2013.
[52] G. Balducci, M. Romeo, M. Stener, G. Fronzoni, D. Cvetko, A. Cossaro, M. Dell’Angela, G. Kladnik, L. Venkataraman, and A. Morgante, “Computational Study of Amino Mediated Molecular Interaction Evidenced in N 1s NEXAFS: 1,4-Diaminobenzene on Au (111),” *J. Phys. Chem. C*, vol. 119, no. 4, pp. 1988–1995, Jan. 2015.